Supporting Information

The surface reactivity of Li_2MnO_3: First principles and experimental study

Ambroise Quesne-Turin[1,2,4], Delphine Flahaut[1,4,*], Laurence Croguennec[2,4], Germain Vallverdu[1,4], Joachim Allouche[1], Youn Charles-Blin[1,4], Jean-Noël Chotard[3,4], Michel Ménétrier[2,4] and Isabelle Baraille[1,4]

[1]CNRS/ Univ. Pau & Pays Adour, Institut des Sciences Analytiques et de Physico-chimie pour l'Environnement et les Matériaux, UMR5254, F-64000 Pau, France

[2] CNRS, Univ. Bordeaux, Bordeaux INP, ICMCB UPR 9048, F-33600 Pessac, France

[3]Laboratoire de Réactivité et Chimie des Solides, CNRS-UMR#7314, Université de Picardie Jules Verne, F-80039 Amiens Cedex 1, France.

[4]RS2E, Réseau Français sur le Stockage Electrochimique de l'Energie, FR CNRS 3459, F-80039 Amiens Cedex 1, France

Corresponding Author

*Delphine Flahaut

delphine.flahaut@univ-pau.fr

The Supporting information contains Figures, Tables and description to complete and precise some points in the main manuscript.

The first paragraph describes the slab model used in order to describe the surface in the first-principal calculations.

The Figure S2 exhibits Auger Electron Spectroscopy nanoprobe analyses performed on the (001) crystal surface before adsorption. A chemical mapping of this surface for the manganese, oxygen, and carbon elements is presented in Figure S3.

The determination of the Mn^{3+} and Mn^{4+} contributions to the Mn 2p core peak spectrum is described and shown in Figure S4.

Mn 3s core peaks of Li_2MnO_3 crystal, before and after SO_2 adsorption are shown in Figure S5. The corresponding O1s, Li 1s and Mn 3p core peaks are presented in Figure S6.

Densities of states (DOS) of the bulk and of the (001)-O and (001)-Li surfaces of Li_2MnO_3 have been provided in Figure S7.

Magnetic moments of manganese atoms for different oxidation states have been computed using MnO, Mn_2O_3 and MnO_2 as reference materials. The results are gathered in Table S1.

1. The slab model

Figure S1 gives a schematic view of the slab model commonly used in order to investigate a surface system in 3D periodic codes such as VASP. Here, the vectors $\vec{a}$ and $\vec{c}$ represent the unit cell used in the calculation. Note that in this case the slab is different from that commonly used to describe the crystallographic structure of the layered oxides A_xMO_2 (A = Li, Na, K), i.e., the structural block MO_2 containing two oxygen atomic layers and one transition metal layer.

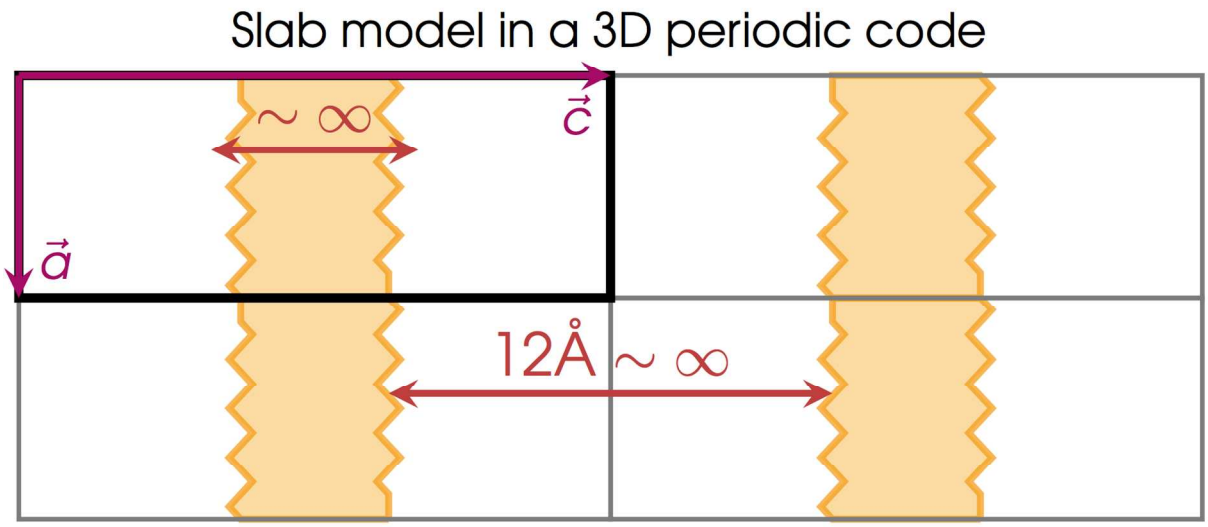

Figure S1. schematic view of the slab model. The periodic unit used in the calculations is defined by the vectors $\vec{a}$ and $\vec{c}$. The orange part corresponds to the material while the white part is vacuum.

Here, the slab is a slice of material corresponding to the smallest crystallographic unit that allows to reproduce both: (i) in its center, the properties of the atoms of an infinite bulk system; (ii) on its edges, the properties of the surface atoms. The slab has therefore to be thick enough to satisfy these conditions but thin enough to be able to run the calculations. The slab surface is perpendicular to a given crystallographic direction and defined by the corresponding Miller indices (hkl). The slab is built by a stacking of atomic layers perpendicular to the given crystallographic direction. Moreover, an empty space has to be introduced on both sides of the slab in the unit cell used for the calculations, in order to make the interactions between two images of the surface vanish in the periodic system.

2. Auger Electron Spectroscopy nanoprobe analyses

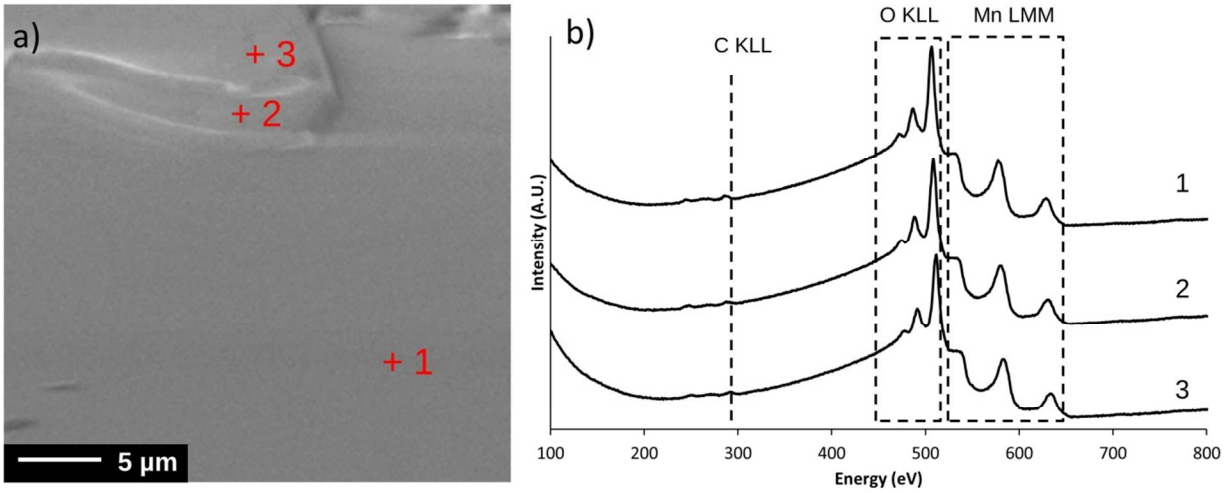

Figure S2. AES analyses of a Li_2MnO_3 crystal before SO_2 adsorption: (a) SEM image with the analyzed target dots (red crosses) with (b) the corresponding Auger spectra.

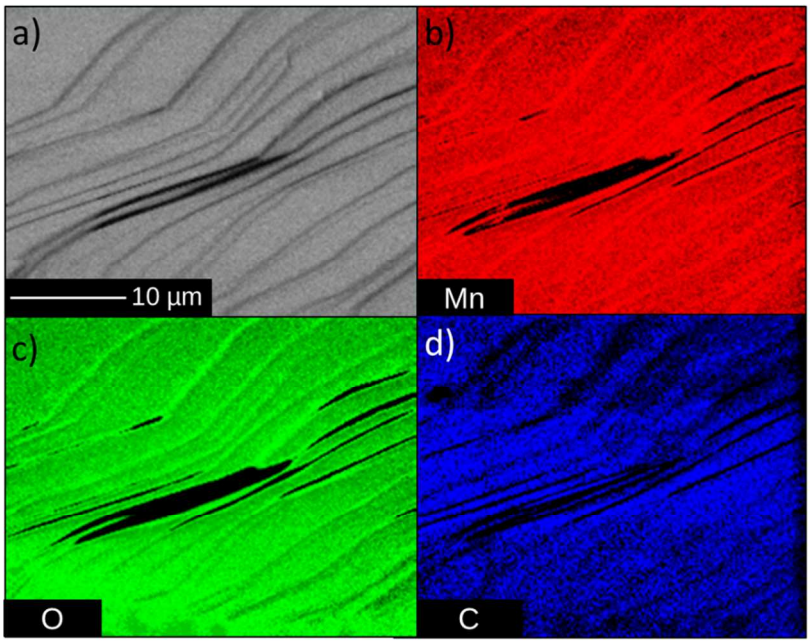

Figure S3. Auger chemical mapping of a Li_2MnO_3 crystal before SO_2 adsorption: (a) SEM image of the analyzed area with the corresponding (b) Mn, (c) O and (d) C maps.

3. XPS Characterization

3.1. Mn 2p core peaks

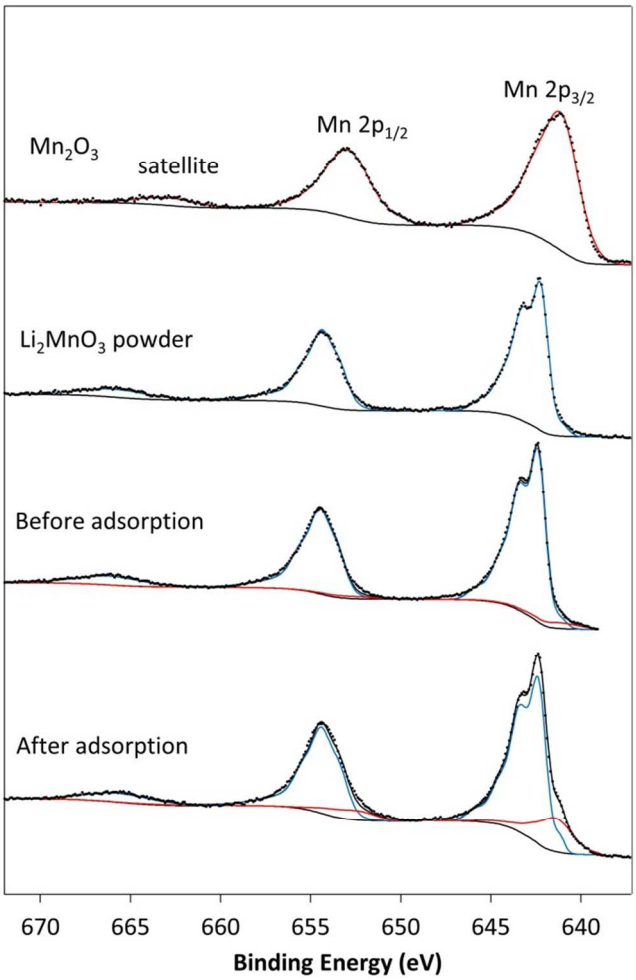

Figure S4. Mn2p core peaks of reference materials, Mn_2O_3 (Mn^{3+}) and Li_2MnO_3 (Mn^{4+}) powder, compared to those of the Li_2MnO_3 crystal, before and after SO_2 adsorption. The Mn^{4+} and Mn^{3+} components used to fit the experimental Mn 2p spectra recorded for the Li_2MnO_3 crystal (before and after adsorption) are the experimental spectra recorded for the Li_2MnO_3 powder (blue line) and for Mn_2O_3 (red line), respectively

The **Error! Reference source not found.** presents Mn2p core peaks of reference compounds, Mn_2O_3 and Li_2MnO_3 as powders, corresponding respectively to high spin Mn^{3+} and Mn^{4+} in octahedral fields as in Li_2MnO_3 crystal. The Mn_2O_3 Mn 2p core peak has a Mn $2p_{3/2}$ maximum at 641.1eV and a Mn $2p_{1/2}$ maximum at 652.9 eV and its satellite at 665 eV. The Li_2MnO_3 Mn 2p core peak has a Mn $2p_{3/2}$ maximum at 642.3 eV and a Mn $2p_{1/2}$ maximum at 654.5 eV eV and its satellite at 666.2 eV. The Li_2MnO_3 crystal Mn 2p core peaks obtained before and after SO_2 adsorption are shown in **Error! Reference source not found.**, their decomposition was performed considering the experimental spectra recorded for the reference materials, with a position constrain of ± 0.2 eV, a full width at half maximum constrain of ± 10% and an area constrain of ± 10%. Thus, the proportion of Mn^{3+} and Mn^{4+} could be determined.

3.2. Mn 3s core peaks

The Figure S5 shows the Mn 3s core peak of crystal before and after SO_2 adsorption. Actually, the exchange interaction of Mn 3s and 3d electrons leads to two photoemission final states and to a splitting of the Mn 3s peak in two components for which the B.E. splitting value is directly relied to the Mn oxidation state. The B.E. splitting, for Mn^{4+}, Mn^{3+} and Mn^{2+} are respectively 4.5 eV, 5.5 eV and 6.5 eV[1,2]. The splitting is 4.5 before adsorption and 4.8 eV after adsorption.

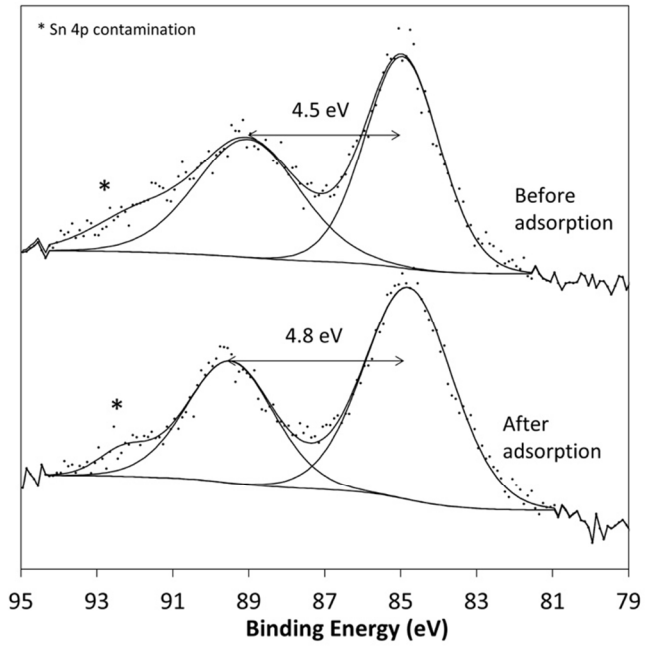

Figure S5. Mn 3s core peaks of Li_2MnO_3 crystal, before and after SO_2 adsorption.

3.3. O 1s and Mn 3p core peaks

The O 1s spectrum given in Figure S6 exhibits three contributions, the first at ~529.7 eV which is associated to the structural oxygen anions, the second at ~531.5 eV which corresponds to the oxygen anions of the extreme surface with a deficient coordination[1] and the third at ~533 eV which is attributed to the oxygen atoms issued from absorbed species. Only the structural oxygens are used to calculate the material stoichiometry. The Li 1s core peak exhibits a peak at 54.4 eV associated to Li^+ in Li_2MnO_3 (Figure S6). The stoichiometry obtained from XPS analysis is $Li_{1.3\pm0.3}MnO_{1.9\pm0.1}$.

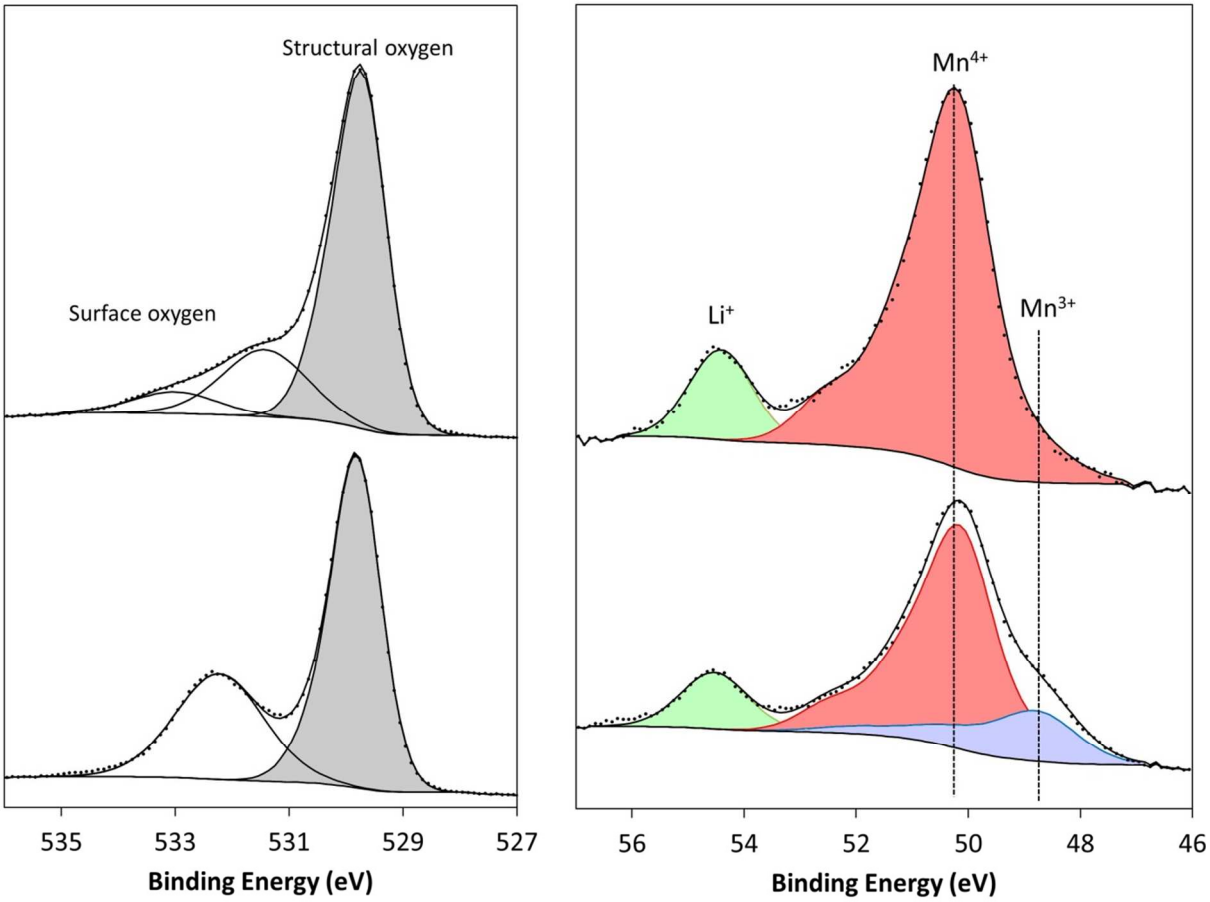

Figure S6. O 1s core peaks (left) and Li 1s and Mn 3p core peaks (right) of Li_2MnO_3 crystal, before (top panel) and after (bottom panel) SO_2 adsorption.

4. Manganese magnetic moment

The aim of the following calculations is to provide a magnetic moment scale in order to be able to describe the formal oxidation degrees of manganese atom in the studied material. Although, these formal charges do not reflect the total electronic density surrounding an atom, they are common tools in order to describe redox processes taking place. Moreover, the magnetic moments are good descriptors of these formal charges. Thus the values obtained below were used as reference values for the considered oxidation degrees of manganese atoms.

The results given hereafter have been obtained with VASP, at the same calculation level than those previously described for Li_2MnO_3 in the main part of the paper. We used a PAW

formalism and the GGA DFT functional proposed by Perdew and Wang,[2,3] with plane waves values of 700eV. The Hubbard-U model is the Dudarev implementation with a U_{eff} parameter of 5 eV.

The MnO, Mn_2O_3, and MnO_2 materials are characterized by manganese atoms in octahedral sites, respectively at the +II, +III and +IV oxidation state. The k-points grids used were a mesh of 3 × 3 × 3 for MnO and Mn_2O_3, and of 3 × 3 × 6 for MnO_2.

	MnO [4]		Mn_2O_3 [5]		MnO_2 [6]	
System	Cubic		Orthorhombic		Tetragonal	
Space group	225 ($Fm\bar{3}m$)		61 (Pbca)		136 ($P4_2/mnm$)	
a (Å) theoretical | exp.	4.509	4.446	9.583	9.416	5.186	4.398
b (Å) theoretical | exp.	4.509	4.446	9.610	9.423	5.081	4.398
c (Å) theoretical | exp.	4.509	4.446	9.611	9.404	2.933	2.873
γ	90		90		90	
μ_B (Mn)	4.7		4.1		3.4	

Table S1. Lattice parameters of calculated MnO, Mn_2O_3 and MnO_2 materials and the manganese atoms magnetic moment.

5. Densities of states (DOS)

Figure S7 presents the DOS of the bulk (top panel) and the two bare slabs: (001)-O and (001)-Li surfaces. Positive and negative DOS correspond to the DOS of up (α) and down (β) electrons respectively. The total DOS are depicted in gray. The green curves are the projected DOS on all manganese atoms of the bulk (in the bulk case) or on one manganese atom at the center of the slab (for the (001)-O and (001)-Li surfaces). The DOS of those manganese atoms

are closed each other which indicates that the bulk properties are properly reproduced at the center of the slab and that manganese atoms can still be interpreted as Mn^{4+} species. Finally, looking at the red curves, corresponding to the projected DOS on a manganese atom on the subsurface layer of the (001)-O and (001)-Li surface models, one can see that the DOS remains closed to the DOS of a bulk manganese atoms excepted a small contribution close to the fermi level corresponding to the usual surface states. Here again, the electronic structure of the manganese atoms on the subsurface layer is not strongly impacted by the formation of the (001) surface and can be associated to Mn^{4+} species.

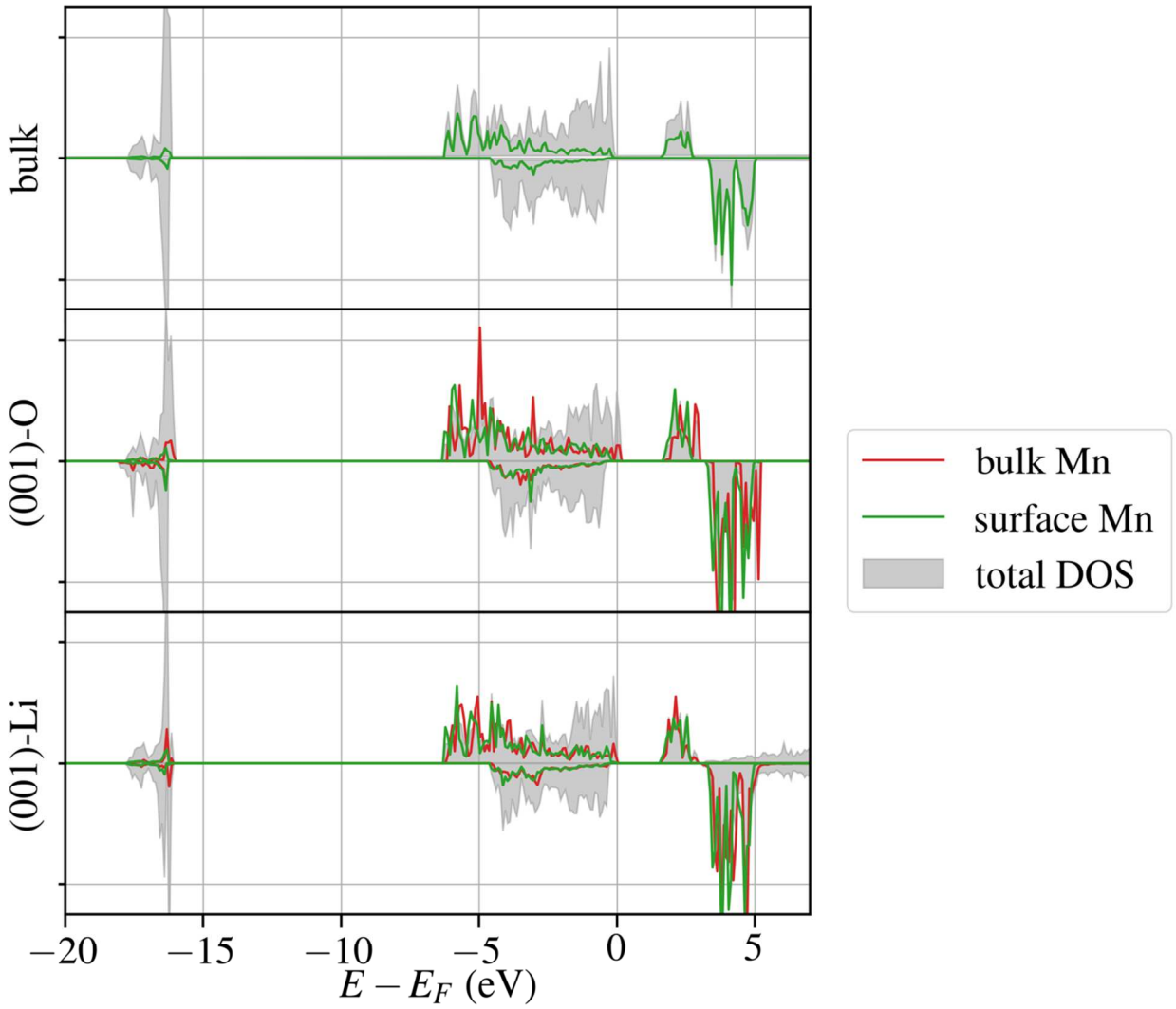

Figure S7. Densities of states (DOS) of the bulk (top panel), the (001)-O surface (middle panel) and the (001)-Li surface (bottom panel) of Li_2MnO_3. The gray filled curves correspond to the total DOS ; the green curves are the projected DOS on all manganese atoms in the case of the bulk and the projected DOS on a manganese atom at the center of the slab for surface models ; The red curves are the projected DOS on a manganese atom on the subsurface layer of the slab models.

REFERENCES

[1] Dahéron, L.; Martinez H.; Dedryvère R.; Baraille I.; Ménétrier M.; Denage C.; Delmas C.; Gonbeau D. Surface Properties of $LiCoO_2$ Investigated by XPS Analyses and Theoretical Calculations. *J. Phys. Chem. C* **2009,** 113**,** 5843–5852.

[2] Perdew, J. P.; Chevary J. A.; Vosko S. H.; Jackson K. A.; Pederson M. R.; Singh D. J.; Fiolhais C. Atoms, Molecules, Solids, and Surfaces: Applications of the Generalized Gradient Approximation for Exchange and Correlation. *Phys. Rev. B* **1992**, 46, 6671–6687.

[3] Perdew, J. P.; Wang, Y. Accurate and Simple Analytic Representation of the Electron-gas Correlation Energy. *Phys. Rev. B* **1992**, 45, 13244–13249.

[4] Sasaki, S.; Fujino, K.; Takéuchi, Y. X-Ray Determination of Electron-Density Distributions in Oxides, MgO, MnO, CoO, and NiO, and Atomic Scattering Factors of their Constituent Atoms. *Proc. Jpn. Acad. Ser. B* **1979**, 55, 43–48.

[5] Geller, S. Structure of α-Mn_2O_3, $(Mn_{0.983}Fe_{0.017})_2O_3$ and $(Mn_{0.37}Fe_{0.63})_2O_3$ and Relation to Magnetic Ordering. *Acta Crystallogr. B* **1971,** 27, 821–828.

[6] Baur, W. H. Rutile-type compounds. V. Refinement of MnO_2 and MgF_2. *Acta Crystallogr. B* **1976,** 32, 2200–2204.